NEUTRON AND TRITIUM EVIDENCE IN THE ELECTROLYTIC REDUCTION OF DEUTERIUM ON PALLADIUM ELECTRODES

TECHNICAL NOTE

KEYWORDS: *cold fusion, electrolysis, radiation*

D. GOZZI, P. L. CIGNINI,* and M. TOMELLINI+ *Università "La Sapienza" Dipartimento di Chimica, P. le Aldo Moro 5, 00185 Roma, Italy*

S. FRULLANI, F. GARIBALDI, F. GHIO, M. JODICE, and G. M. URCIUOLI *Istituto Superiore di Sanità and Sezione INFN-Sanità Laboratorio di Fisica, Viale Regina Margherita 299, 00161 Roma, Italy*

Received April 24, 1991
Accepted for Publication June 24, 1991

A Fleischmann and Pons type experiment was carried out for ~3 months in a ten-cell electrochemical system. All the cells were connected in series, and electrolysis was performed in galvanostatic mode at a maximum current of 2.5 A, corresponding on the average to 500 mA/cm^2. In this experiment, all cathodes were made of palladium, and the anodes were made of platinum. In nine cells out of ten, the cathodes were shaped into parallelepipeds (25 × 5 × 5 mm^3) by high-vacuum sintering according to a previously reported procedure. The starting material for all these electrodes was palladium sponge powder. The tenth cathode was made of 32 short 0.5-mm-diam palladium wires, gold welded together at one end. A similar concentration of screw dislocations was produced in each wire. Three different groups of sintered cathodes were used in the experiment, corresponding to three different sintering procedures. Nine cells contained 0.2 M LiOD in D_2O as electrolyte. The tenth cell, containing a sintered cathode, was in 0.2 M LiOH in H_2O.

Measurements of neutrons, tritium in the solution and in the recombined gases, gamma rays, and electrode temperature were carried out. When the current density reached the highest values, a marked increase of the neutron detector count rate with respect to the background level (2 count/h) was observed. The emissions occurred in bursts. This behavior was observed for ~10 days but only when the current density was set at >320 mA/cm^2. In the first part of that period, an excess of tritium with respect to the expected value calculated for the electrolytic enrichment was found in three cells out of nine (one of the cells was in light water). This excess was about twice the amount expected with respect to the enrichment and about four times the initial tritium content in the heavy water (267 decay/min·ml). The other cells, including the one in light water, did not show any excess tritium, the value of which was in good agreement with the calculated value. Some aspects concerning the thermal behavior of the electrodes are also discussed.

INTRODUCTION

Research on cold fusion began in April 1989 following the claims of two research groups[1,2] concerning the occurrence of nuclear reactions in condensed matter by infusing deuterium in palladium or titanium by means of electrolysis in heavy water electrolytic solutions. This paper shows the work related to a second generation of experiments.

The first-generation experiments are described elsewhere.[3-8] The second generation of experiments is based on a multicell apparatus in which several experiments along the Fleischmann-Pons line can be carried out simultaneously by measuring electrochemical, thermal, and nuclear quantities in a well-controlled automatic system. The first-generation experiments were done in single cells.

Two cooperating groups were and are still active in the field: one composed of physical chemists from the Department of Chemistry of the Università "La Sapienza" and CNR Centro di Termodinamica Chimica alle Alte Temperature located in the Department of Chemistry and the other group composed of nuclear physicists from the Physics Laboratory of the Istituto Superiore de Sanità and Sanità unity of the National Institute of Nuclear Physics.

Our work has focused on finding time correlations among as many independent experimental variables as possible because we believe that this is the best way to develop this matter in a scientifically significant way. The results presented in this paper were obtained in light of this approach.

*Current address: CNR, Centro di Termodinamica Chimica Alte Temperature, % Dipartimento di Chimica, P. le Aldo Moro 5, 00185, Roma, Italy.
+Current address: Dipartimento di Scienze e Tecnologie Chimiche, Universita di Roma "Tor Vergata," Via O. Raimondo, 00173, Roma, Italy.

EXPERIMENTAL

The features of our experimental system can be summarized as follows:

1. Ten cells are placed according to a decagon ideally contained in a perpex torus in which high-speed thermostated water circulates.

2. Such a geometry allows the neutron counter to be placed in the center of the torus and the external gamma detectors to be placed in diametrally opposite positions.

3. All the cells are electrically connected in series. Under galvanostatic conditions (I = constant), the current crossing all cells is the same. According to Faraday's law, the D_2O volume that is electrochemically converted is the same in all cells. This implies two fundamental aspects: (a) In principle, cells constructed to be equal must show equal thermal effects due to the same electrical input power, and (b) because of the mass balance of tritium and its electrolytic enrichment, the isotope concentration must be the same in each cell.

4. Gases produced by each cell are catalytically recombined to determine the amount of tritium in the gaseous phase.

5. An automatic device allows the electrolyte level in each cell to be kept constant by adding D_2O as needed.

6. The cathode versus anode and cathode versus reference voltages as well as the temperature of the cathode are measured.

7. One of the ten cells contains the electrolyte diluted in H_2O instead of D_2O. This gives a blank for all the quantities measured. Particularly, as is stressed later, this is a good way to determine whether tritium is released by the cathode and/or the materials of the cell.

8. There is a $D_2(g)$ [$H_2(g)$ for the cell in H_2O] inlet to perform the *in situ* charging of the cathode at the start of the experiment before the introduction of the electrolyte solution.

Therefore, the quantities measured *separately* in each cell are as follows:

1. cathode versus anode voltage
2. cathode versus reference voltage
3. tritium activity in the electrolyte
4. tritium activity in the gaseous phase
5. temperature of the cathode
6. D_2O (H_2O) consumption.

The gamma radiation spectra and the neutron emission measurements are *common* to all the cells. Especially in the neutron emission measurement, this is a serious limitation that might be eliminated with a suitable neutron counter. All these quantities are continuously monitored except the tritium activity, which is measured by a systematic sampling of the electrolyte solution and recombined water.

Tritium measurements are carried out by the liquid scintillation method on a Beckmann LS 1801 apparatus according to the procedure suggested by the international standards; most are done automatically by the apparatus itself. In particular, the procedure adopted requires the measurement to start 2 h after the liquid scintillator (12.5 ml) is mixed with the sample (1.00 ± 0.02 ml), to eliminate chemiluminescence.

Other quantities measured are the current applied, the temperature of the circulating water at three points of the torus, and the temperature of the catalyst of each recombiner.

Data Acquisition System

Data acquisition is a prominent aspect of this kind of experiment and must be done with great care. The study of the base software and the planning, writing, the testing of the program were time-consuming. The data acquisition system is based on the following components:

1. dedicated software written by the LabVIEW base software by National Instruments
2. programmable data logger, a Solartron 3531 D, with 40 analog channels [direct current (dc), alternating current (ac), voltage and current, several types of thermocouples, two or four probes for resistance], 20 digital input channels, 20 digital output channels, 20 event channels at 500 Hz, 5 counter channels at 400 kHz, and 5 analog output channels. Embedded peripherals include a $3\frac{1}{4}$-in., 800 kilobyte drive and printer as well as IEEE-488 and RS-232 interfaces.
3. Macintosh IIx computer with 8-megabyte random access memory, 60-megabyte hard drive, $3\frac{1}{4}$-in., 2-megabyte drive, and NB-DMA-8G board interface IEEE-488 by National Instruments.

The main features of the data acquisition architecture can be summarized as follows:

1. The data logger provides direct readings of all the signals, except those coming from the gamma detectors, which have a separate data acquisition system, by a cyclic repetition of programmed tasks (up to eight) scanning the channels.

2. Because of the long times required to perform this kind of experiment, it would be practically impossible to store and handle the data if the channels were continuously scanned. To avoid this, a sentinel task not transmitting to the IEEE-488 interface continuously scans all the channels while a task that does transmit to the IEEE-488 works at a lower frequency. If one of these channels is found to be in alarm status, the lower frequency task is aborted, and a high-frequency task is triggered to scan the same channels. Generally, the alarm is set on the channels reading the temperature of the cathodes and the count rate of the neutron counter.

3. The neutron counter signal after transistor-to-transistor logic conversion is connected in parallel to (a) three event channels with 2-ms (500-Hz) time resolution (dating, count rate, and total counts), (b) a counter channel for the total count at a maximum frequency of 400 kHz, (c) an external LeCroy 4604 counter for the total count at a maximum frequency of 125 MHz, and (d) a digital oscilloscope-printer system to control the pulse shape.

4. Two of the eight data logger tasks are reserved for the control and detection of the time intervals between the openings and closings of the electrovalves that allow the water refilling in each cell. Since the flow rate is known, the water consumption is given by its product by the summation of all the intervals.

The homemade software also allows the following to be displayed in real time: (a) the differences between two of the ten cells in both the cathode temperatures and the voltage cathode versus anode or cathode versus references, (b) the

TABLE I

Approximate Gamma-Ray Detector Efficiency

Detector	Closest Cells	Farthest Cells
NaI(Tl)	10^{-3}	10^{-4}
HPGe	10^{-5}	10^{-6}

count rate and the total counts of the neutron counters at both 500 Hz and 400 kHz, and (c) the water consumption for each cell.

The nuclear instrumentation consists of the following:

1. Two detectors for gamma radiation emission: a large NaI(Tl) monocrystal with high efficiency ($10 \times 10 \times 40$ cm^3) and a high-purity germanium (HPGe) detector with a cylindrical germanium monocrystal 49.0-mm diam $\times$ 63.1 mm at high resolution [full-width at half-maximum = 1.68 keV for 1.33 MeV from a ^{60}Co source; for the same source placed 25 cm from the detector, the relative efficiency is 22% with respect to a 3-in.-diam NaI(Tl) detector]. The two detectors are placed at the periphery of the torus in opposite positions. The detection efficiency is strongly dependent on the geometry. For the 2.225-MeV gamma ray generated by the ($n + p = d + \gamma$) process, if neutrons are emitted by the cathodes, the efficiency of the detectors depends on the position of the cells containing them. Table I shows the approximate efficiency values for both detectors.

2. The data acquisition occurs through ORTEC electronics on Maestro II software, which allows independent displays of the gamma spectra of the respective detectors. Spectra are automatically acquired and stored by adopting time intervals between 8 and 36 min.

3. A ^{3}He neutron counter moderated by polyethylene from which an analog and a digital signal are taken.

All the apparatuses are supplied by a 3 kV·A backup group (Emerson AP 161), which produces a filtered and levelled 220-V ac line. Figure 1 shows a general diagram of the experimental apparatus.

The torus containing the cells, gamma-ray and neutron detectors, and some ancillary devices are placed in a Faraday cage ($186 \times 186 \times 203$ cm^3) to reduce the electromagnetic noise as found by the measurement of the electric and magnetic fields inside and outside.

Preparation of the Electrodes

Cathodes

All ten cathodes are made of palladium. Nine were prepared from palladium sponge (Johnson & Matthey) by sintering the pressed specimens obtained in a stainless steel die. The specimen dimensions were $25 \times 5 \times 5$ mm^3. The general sintering procedure is described elsewhere.[5,7] Three different procedures were adopted, producing three groups of samples, G_1, G_2, and G_3. The tenth cathode, G_4, was formed of thirty-two 0.5-mm-diam $\times$ 25-mm palladium wires, all gold-welded at one end. This number of wires gave a palladium mass comparable with the other cathodes. Each wire was treated in such a way as to have a similar concentration of screw dislocations.

For every cathode, the current leads were the metal shields of the K-type thermocouple (electrically insulated by the thermoelement), which were welded to the cathode. The junction zone was protected by an epoxy resin that had been confirmed to be resistant to the strongly alkaline electrolyte solution.

Anodes

All anodes were 1-mm-diam wire shaped as a 12-mm-diam $\times$ 30-mm-long cylindrical spiral in such a way that the cathode was placed along its major axis.

Electrolyte

The electrolyte was either a 0.2 *M* LiOD or LiOH solution with D_2O or H_2O as solvent. Each cell contained up to 31 ml of electrolyte solution. In cell 8, the electrolyte was LiOH in H_2O.

Cells

Figure 2 shows a detailed schematic of the cell utilized in the experiment. The number of the cells, in parentheses, and their respective groups are as follows: G_1(1,2), G_4(3), G_2(4,5,6,7), and G_3(8,9,10).

Experimental Procedure

The length of a single data acquisition period is conditioned by the dimensions of the matrix of the data compatible with the software. Typically, the scanning interval of the data logger was set each 5 min. In some cases, this time was doubled or halved. If one or more alarms were activated, the scanning interval became 20 s. The typical length of an acquisition period was 83 h. The acquisition of the gamma spectra generally occurred for both the detectors each 24 min. For the neutron emission, the acquisition interval was set by the data logger according to the procedure discussed earlier.

The pulse shape of the neutron counter was also recorded by a printer connected to an HP 52501 A digital oscilloscope. Figure 3a shows the pulse shape of a thermalized neutron coming from the Am-Be neutron source as *seen* by the counter. A different shape having also a positive part was shown every time a pulse from the neutron counter was induced by a simulated electromagnetic noise (Fig. 3b).

Sampling for Tritium Determination

At more or less equal time intervals, 1 ml of electrolyte was sucked from each cell by a 1-ml pipette (a pipette for each cell to avoid contamination) and put in a plastic container carrying the cell number identification and date.

RESULTS

Current Density versus Neutron Emission

Figure 4a shows the time sequence by which the current was changed during the entire experiment. It was gradually increased starting from 50 mA, corresponding to 10 mA/cm^2, by considering a mean cathode surface area of 5 cm^2 and maintaining each current value for long times. This procedure was adopted in light of the Texas A&M University experiments,[9] and it probably enables a higher deuterium/palladium (D/Pd) ratio.

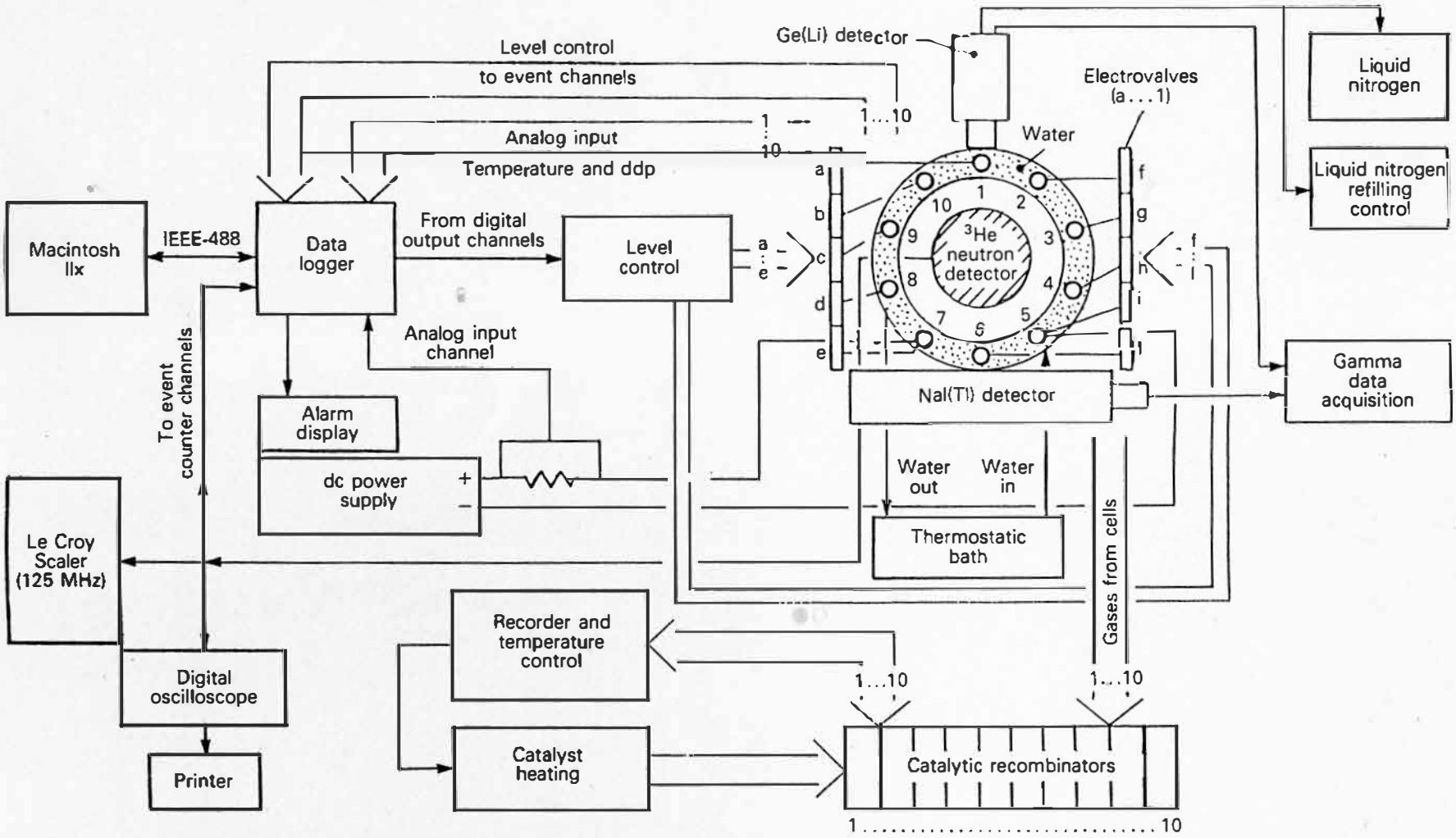

Fig. 1. General schematic of the experimental apparatus.

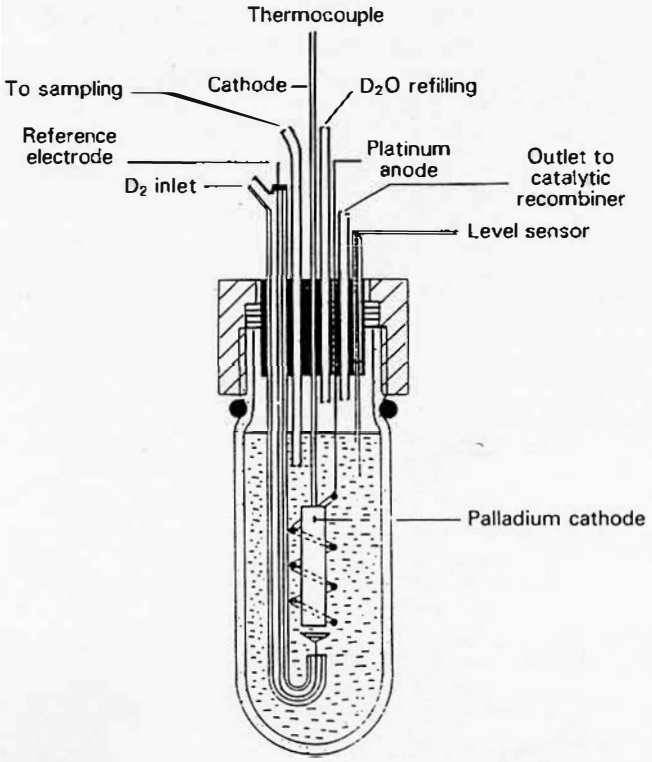

Fig. 2. The electrolysis cell. The size, materials, and masses are the same in all ten cells.

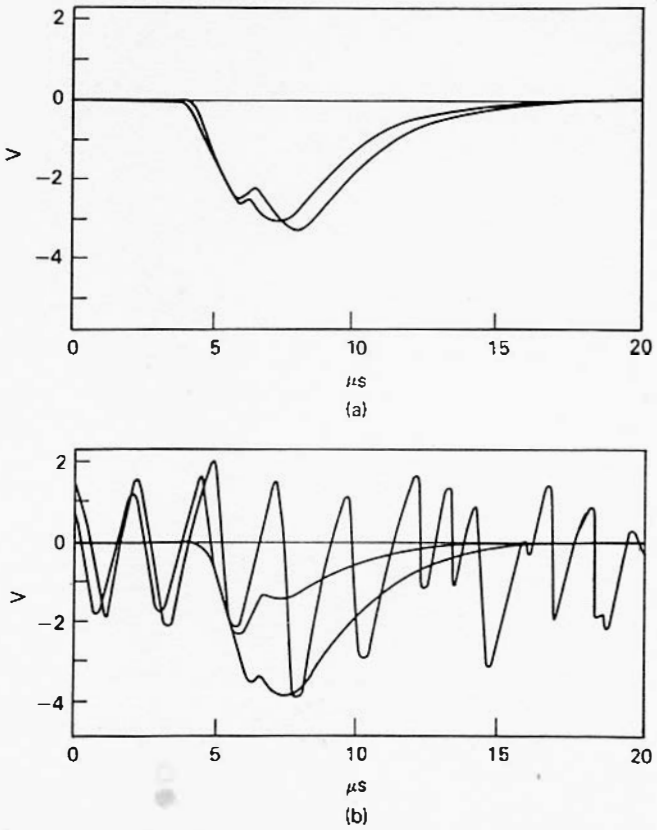

Fig. 3. Oscillographic traces generated by the ^3He neutron counter when (a) an Am-Be neutron source was placed close to the counter and (b) a simulated electromagnetic noise was induced on the counter.

The maximum current density reached was 500 mA/cm^2. The highest limit applicable depends on the power supply characteristics as well as the total voltage drop through the cells.

The electrolyte resistance generally increases as the concentration in the electrolyte solution decreases. During the experiment, we observed that after long-lasting electrolysis, especially at high current density, the lithium concentration in the electrolyte solution decreased. An explanation of this behavior lies in the fact that the solvent H_2O or D_2O was systematically added while the electrolytic solution was carried by the evolving gases out of the cells through microdrops. The final result of these two actions was dilution. We did lithium determinations by plasma atomic absorption spectroscopy after a passed electric charge equal to $\left(\int I dt\right)/F = 36.65$ mol (1 F = 96487 C·mol^{-1}). Lithium concentrations, cell voltages, and electrode temperatures at the time of the sampling are shown in Table II.

Except for cell 8 (with H_2O), there is a certain trend between the ΔV_i increase and decrease of lithium concentration in the electrolyte. The temperature values would obviously be expected to follow the same trend provided that the electrolyte volumes were the same for all cells if no energy excess is produced. As we show later, it was necessary to manually add solvent to some cells to compensate for excess consumption due to an unexplained temperature increase.

Figure 4b shows, on the same time scale, the neutron

TABLE II

Electrolyte Sampling*

	Cell									
	1	2	3	4	5	6	7	8	9	10
Lithium content ($\times 10^2/M$)	6.76	9.94	10.0	12.4	9.09	5.48	3.24	6.71	6.94	9.26
$-\Delta$(Li) (%)	66.2	50.3	49.9	37.8	54.5	72.6	83.8	66.4	65.3	53.7
$-\Delta V_i/V$	16.7	12.2	14.0	12.0	12.7	18.7	19.0	5.61	13.4	12.7
T (°C)	53.6	46.5	48.9	45.0	48.0	65.8	60.9	49.6	46.9	44.8

*11:00 A.M., May 25, 1990; I = 2200 mA; thermostat temperature = 22°C.

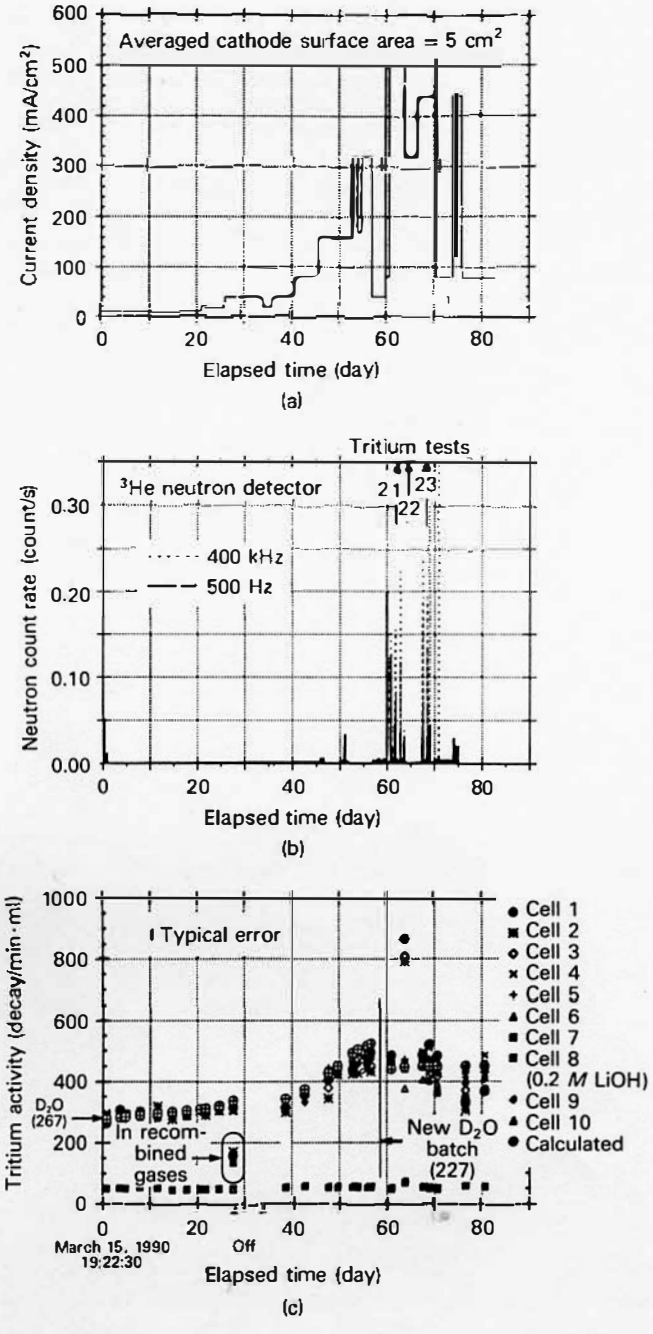

Fig. 4. Applied current density profile, neutron count rate, and tritium activity in all cells throughout the experiment. The tritium values shown have not been corrected for the instrumental background, which was equal to the values reported for cell 8 in H_2O.

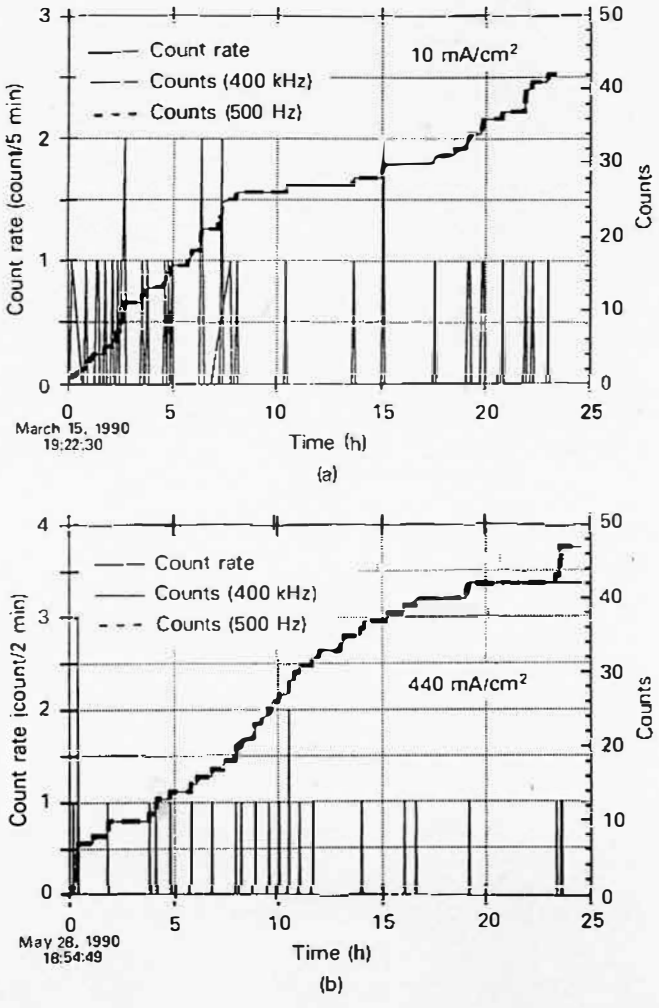

Fig. 5. Typical behavior of the count rate and count of the background neutrons as obtained by the counters at 500 Hz and 400 kHz: (a) March 15, 1990, at the beginning of the experiment and (b) May 28, 1990, a few days before the end of the experiment.

count rate as obtained by the two counters at 500 Hz and 400 kHz. For ~2 months, the two counts were practically the same and equal to the background detected for ~1 yr by using the same apparatus. The background was between 1.5 and 2 count/h ($4.2 \div 5.5 \times 10^{-4}$ s^{-1}).

Figure 5 shows, as an example, the typical trend of the count rate and integral count in two different periods of the experiment and in different experimental conditions. It is important to observe that in this figure there is a perfect superimposition of the integral count curves independent of the working frequency of the counter.

A comparison of the plots in Figs. 4a and 4b shows the following:

1. There is a correlation between the neutron emission and current density.

2. The phenomenon began when the current density was set at the maximum value.

3. In this case, the ratio between the high- and low-frequency counts was initially roughly equal to 1 but increased with time.

4. The correlation with the current density seems to display a threshold at 320 mA/cm². In fact, for three distinct periods, the current was set at that value before and after the beginning of the phenomenon without any significant change in the count rate.

A direct observation was made for several hours by one or more investigators during the period characterized by the increase of the neutron count rate. A peculiar phenomenon was the characteristic way in which the signals followed one another. Many of the counts were concentrated in very short times, lasting a few seconds or less, by fast sequence, having an increasing number of counts, followed by pauses ranging from some minutes to >10 h. This emission structure is very similar to the burst structure found by other groups in nonelectrochemical experiments.[10]

Unfortunately, our pulse-shape discrimination system was not able to print the shape of each pulse of the neutron counter when the time between two signals was less than the time necessary to print the hardcopy of the oscilloscope screen. This time is ~40 s. Therefore, we are not able to claim that the increase in the count rate is to be attributed solely to neutrons. In fact, while many pulses were similar to those shown in Fig. 3a, others had shapes either like those of Fig. 3b or some hybrid shape as shown in Fig. 6.

We believe that the count at 500 Hz is closer to the true number of emitted neutrons because the typical shape of a noise-induced signal has a greater effect on the higher frequency counters. Concerning signals having an irregular shape, we have to assume that they were spurious but generated by the electrochemical cell system itself. This was apparent during the experiment when the probe of one of the oscilloscope channels was put into contact with the wire connecting all the cell electrodes, the ends of which started from the terminals of the power supply, because a weak damped ac signal was observed at the same time. This signal was observed every time the pulse shape was not the one expected from a neutron. Therefore, it seems that one or more cells generated noise. It is opportune to point out that this hypothesis is essentially based on three reasons:

1. During the entire experiment, great care was taken that any device, other than the experimental apparatus, in the laboratory or nearby, that was potentially able to produce noise on the neutron counter was activated. At different times and under different meteorological conditions, all apparatuses in the nearby laboratories were switched on and off many times to test the neutron counter response. We never obtained correlated effects. Some devices in the laboratory were found to be noise sources when activated or deactivated, such as neon lamps and the air conditioning system. We substituted the neon lamps with incandescence lamps, turned off the air conditioning, and maintained the other devices.

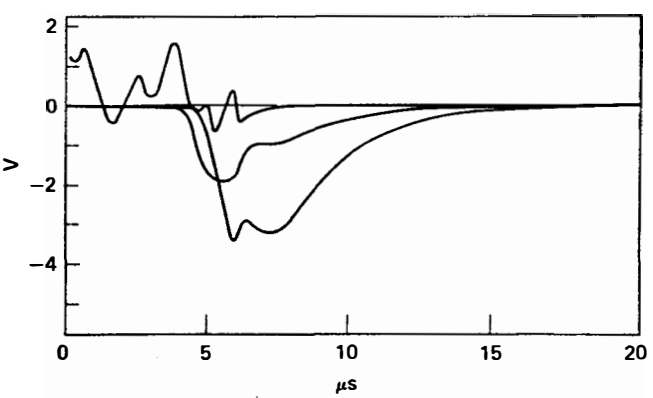

Fig. 6. Oscillographic trace of an anomalous pulse superimposed on the trace of a regular neutron signal.

2. The power supply cannot be a noise source because of its high-quality electronic characteristics and because the following check was done at the end of the experiment. The total voltage drop of all the cells was substituted by a Ni-Cr 70-Ω resistance maintaining the same geometry of the electrical line with respect to the neutron counter. Current values up to 2.5 A were set without observing any change in the neutron count rate with respect to the background.

3. Very near our laboratory, there is a group that systematically and continuously acquires cosmic-ray data. We examined their recordings corresponding to the period relevant to our experiment, and we found no significant change in the cosmic background.

Two hypotheses on the mechanism of the cold fusion are fracture[10] and the formation of dendritic structures onto the cathode surface,[11] which both suggest microplasma generation through a very high electrical field that is localized, in the fractures, or between the dendrites. In both the cases, we are in the presence of electrical fields rapidly changing in time to which an electromagnetic signal could be associated. The burst structure observed may be consistent with such mechanisms even if they are not the mechanism generating nuclear products.

Neutron Emission Versus Tritium Production

Figure 4c gives the tritium activity in all the cells. The solid squares in the lower part of the figure, corresponding to the cell containing H_2O (cell 8), represent the instrumental background of the measuring apparatus, which remained constant throughout the experiment. No appreciable change was found between the results obtained on pure liquid scintillator and those for liquid scintillator plus electrolyte from cell 8.

The cross-circles represent the calculated value of the isotopic enrichment due to the electrolysis. This calculation is of fundamental importance to establish whether tritium is produced by a nuclear process. It is based on the tritium mass balance in the experimental condition to keep the volume of the electrolyte constant.[12] In our case, such a condition was always satisfied through the automatic water refilling device, except for certain occasions where excessive water consumption occurred because of evaporation.

The tritium mass balance in any cell can be written as follows:

$$\mathrm{DTO}_{\mathrm{D_2O}} = (\mathrm{DT} + \mathrm{DTO})_{gas} \ , \qquad (1)$$

where the left term represents tritium input as DTO in the cell through D_2O. The right side term is the tritium output through the DT gaseous molecule, produced by the electrolysis, and DTO vapor, which together with D_2O saturates the gaseous phase.

The equation obtained allows calculation of the DTO molar fraction x, corresponding to the D_2O electrolyzed moles n_E, as

$$x = \alpha - (\alpha - x_0)\exp(-\beta t) \ , \qquad (2)$$

where

x_0 = initial molar fraction in the electrolyte solution

$\alpha = aA/B$

$\beta = Bn_E/N$

$A = \{1 + [P_v/2(P - P_v)]\}$

$B = \{(1/\lambda_E) + [P_v/2\lambda_v(P - P_v)]\}$

a = DTO molar fraction in the D_2O feed (initially equal to 267 decay/min·ml and 227 decay/min·ml in a second batch)

N = number of D_2O moles = $(V_0\rho/M) = V_0/V_M$

where

V_0 = initial volume of electrolyte

ρ = D_2O density

M = D_2O molecular weight

V_M = molar volume

P_v = D_2O vapor pressure

P = total pressure in the cell

λ_E = electrolytic separation factor, $(T/D)_{liq}/(T/D)_{gas}$

λ_v = isotopic separation factor due to evaporation, $P_v(D_2O)/P_v(DTO)$.

By Eq. (2), when $t \to \infty$, $x = \alpha$, and x is an increasing or decreasing function according to whether $x_0 <$ or $> \alpha$, respectively.

The values of A and B mainly depend on the temperature. If, as in our case, $a = x_0$, Eq. (2) becomes

$$x = x_0\{(A/B) - [(A/B) - 1]\exp(-\beta' Q)\} \quad , \qquad (3)$$

where

$\beta' = B/2\,FN$

$n_E = I/2\,F$ by Faraday's law

I = current

$Q = I \times t$ = charge in coulombs passed at time t.

Therefore, a correct investigation into the tritium enrichment must be carried out with respect to the charge instead of time, unless the current is kept constant throughout the experiment. This did not occur in our experiment (see Fig. 4a).

Furthermore, Eq. (3) shows that when $Q \to \infty$, $x_{lim} = x_0A/B = aA/B = \alpha$.

By Ref. 12, the following equations were obtained by linear best fitting ($R > 0.99$):

$$P_v(D_2O) = 6.21 \times 10^{-4}\exp(5.143 \times 10^{-2}T) \quad , \qquad (4)$$

$$P_v(DTO) = 5.72 \times 10^{-4}\exp(5.165 \times 10^{-2}T) \quad , \qquad (5)$$

and

$$\lambda_v = 1.0857\exp(-2.200 \times 10^{-4}T) \quad , \qquad (6)$$

where pressure and temperature have been converted into SI units, pascals and degrees kelvin, respectively.

By assuming a λ_E value independent of temperature, generally taken as ≈ 2, it is possible to calculate the A/B ratio at any temperature. In the range of temperature of interest, this ratio is, in fact, practically equal to 2. Therefore, according to Eq. (3), if $Q \to \infty$, $x_{lim} \approx 2a$, and Eq. (3) will always be an increasing function. We can conclude that for an electrolysis at constant V_0 and T, the upper limit of tritium enrichment is equal to twice its initial concentration.

By inspection of Fig. 4c, one can see that there is a time correlation between the increase of tritium in cells 1, 2, and 3 and the beginning of the period in which the neutron count rate increased. This was found during tritium test 22, corresponding to the sampling done at 3:00 P.M. on May 18 while the current was set at 2.5 A and Q was 2 410 622 C, that is, 24.98 mol or 133.9 A·h/cm^2. The tritium activity values found in cells 1, 2, and 3 are not comparable with either the electrolytic enrichment or the experimental error. In fact, with respect to test 21, the sampling of which was done at 6:30 P.M. on May 15 at the same current, the tritium concentration increases in the three cells were, respectively, equal to 1.78, 1.74, and 1.77 times. On the other hand, as already stated, a correct examination of the tritium data has to be done versus Q and not versus t. Figure 7 shows the data of Fig. 4c plotted against the electric charge passed instead of the time. This is due only to the fact that current was not kept constant throughout the experiment (see Fig. 4a).

Starting on May 14 when a new batch of D_2O at lower tritium concentration was utilized [a = 227 decay/min·ml (92.4 nCi/kg)], the calculated effect on the mass balance was in a good agreement with the experimental results.

It is interesting to observe that before test 22, the experimental value of tritium averaged on all the cells, except cell 8 in H_2O, was 465 decay/min·ml at $Q = 18.59$ mol. By Eq. (3), the limit value of tritium would be approximately between 267×2 and 227×2, that is, 534 and 454. This value depends only on the temperature, though very slowly, whereas the $\beta' = BV_M/2FV_0$ term at exponential in Eq. (3) depends on both the temperature, through B, and the electrolyte volume V_0. By assuming that B is scarcely influenced by temperature, as given through Eq. (6) for λ_v, the unique term that can significantly influence the attainment of the limit value of the tritium enrichment is V_0, if it were not constant throughout the experiment.

As an example, we can calculate the charge Q necessary to reach a given percentage r of the limit value of the tritium enrichment. To do this, Eq. (3) can be written in the form

$$Q = -(1/\beta')\ln[(100 - r)/100(1 - u)] \quad , \qquad (7)$$

where $u = B/A$. At T and V_0, respectively, equal to 323 K and 31 ml, a charge $Q = 22.95$ mol is necessary to reach $r = 99.95$. At test 22, the mean value of the tritium activity T_{22} in all the cells, except cells 1, 2, and 3, which were clearly out of the enrichment, as well as cell 8, was (440 ± 20) decay/min·ml, which has to be compared with $x_{lim} = 2a = 454$ decay/min·ml. In fact, for that test, the corresponding charge was 24.98 mol greater than the charge necessary to reach the 99.95%, as already shown.

We exclude the following:

1. In test 22, there was an error in the sampling of the electrolyte solution; this occurred only for the first three cells. (Checks were done through the lithium determination in the scintillation cocktail. They confirmed that the lithium concentration was as expected.)

2. Tritium was released by some materials constituting the cells, palladium cathodes included. This was not possible because all the cells were made of the same materials, and all the sintered palladium cathodes (nine out of ten) belonged to the same batch of palladium sponge powder. Furthermore, they were prepared by a high-temperature/high-vacuum process. The evidence that excess tritium was not found in all the cells, including cell 8 (H_2O, sintered cathode), which represents the blank, is a strong argument against contamination. This argument is further supported by the fact that the palladium utilized was a powder that statistically excluded any type of

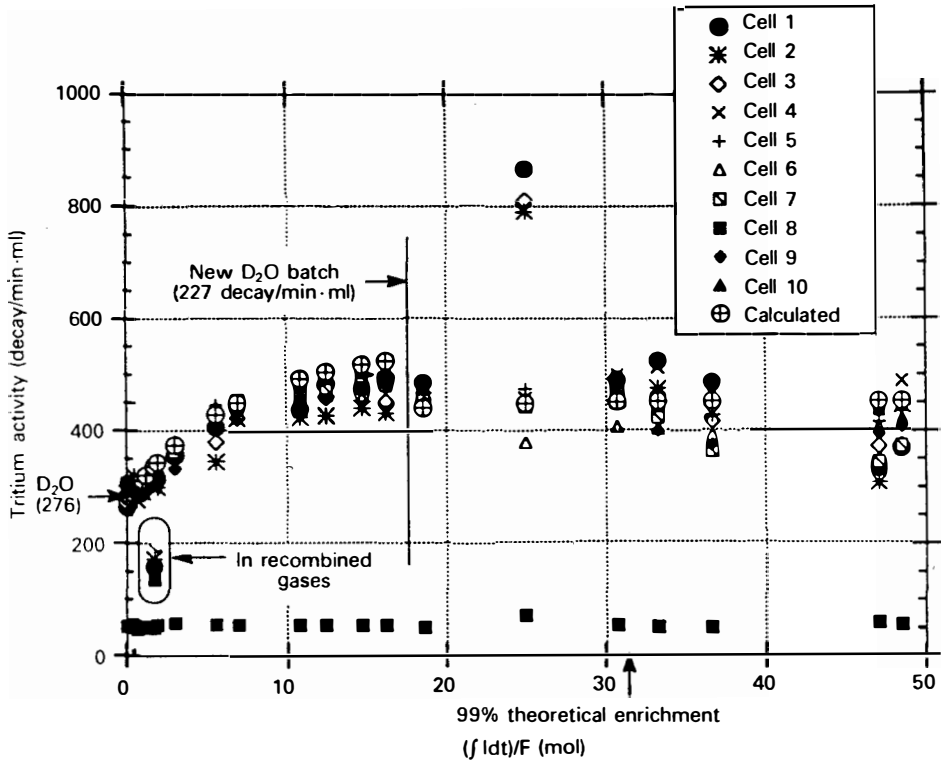

Fig. 7. Experimental and calculated activity (cross-circles) of tritium versus the electrical charge. The values shown have not been corrected by the instrumental background, which was equal to the values reported for cell 8.

spot contamination. Such considerations should be done in light of the recent claims reported in the literature.[13]

We realize that we are not able to find any other convincing explanation to justify the tritium excess found except that a nuclear process occurred.

Because the tritium production occurred in an unknown time interval between tests 21 and 22, that is, between 6:30 P.M. on May 15 and 3:00 P.M. on May 18 (the period in which we observed the increase of the count rate), we can evaluate the tritium activity at that time τ ($\approx$11:00 A.M. on May 16) assuming that the phenomenon began with a burst of a nuclear tritium-producing process. In other words, if we consider the well-known nuclear fusion reactions,

$$d + d = {}^3\mathrm{He}(0.82\ \mathrm{MeV}) + n(2.45\ \mathrm{MeV}) \qquad (8)$$

or

$$d + d = \mathrm{T}(1.01\ \mathrm{MeV}) + p(3.02\ \mathrm{MeV})\ , \qquad (9)$$

and assume that the reaction (9) is simultaneous with reaction (8) for only a short time and then stops, we will observe that the initial tritium concentration produced would decrease with time according to the tritium mass balance in the cell. If it is so, we may ask what its concentration would have been if tritium had been measured at time τ. An answer can be given to this question on the criteria that allowed us to write Eq. (3). In fact, that equation is also the concentration decay of tritium in the case $x_0 > \alpha$, as was expected to happen for cells 1, 2, and 3 between tests 22 and 23. Putting $\alpha = x_{lim} \approx \mathrm{T}_{23}$ (this is consistent with the previous considerations), Eqs. (2) and (3) can be written in the form

$$x = \alpha + (\mathrm{T}_{22} - \alpha)\exp[-\beta'(Q - Q_{21\text{-}23})]\ , \qquad (10)$$

where $Q_{21\text{-}23}$ represents the charge passed between tests 21 and 23, which was equal to 12.15 F. Figure 8 shows that at time τ, the tritium concentration would have been $\approx 5x_{lim}$ or $\approx 10a$. This curve was obtained by the best-fitting curve obtained by Eq. (10) forced to pass on the experimental points of tests 22 and 23.

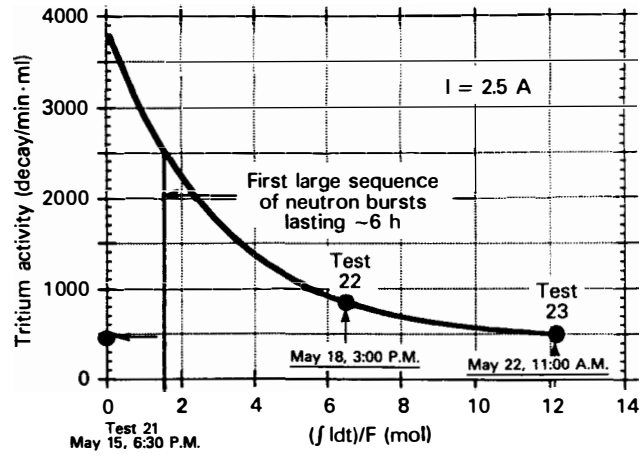

Fig. 8. Best fitting of the decay curve of the tritium activity through the experimental points of tests 22 and 23 for one of the cells that gave tritium excess. If the sampling for the tritium test had been done at the time when the neutron emission increased, the tritium activity would have been five times greater than the expected value.

The excess tritium values are in agreement with some authors,[14] especially the values found by Storms and Talcott[15] at Los Alamos National Laboratory. They do not agree with the values found by Bockris et al.[16] at Texas A&M University and by the group at Bhabha Atomic Research Centre.[12] Both these groups found much higher tritium excesses, up to 4 to 5 orders of magnitude.

From Fig. 4c or Fig. 7, one can see that the unique tritium measurement done on the recombined gases (after a trivial accident destroyed all the recombinators) was in good agreement with the λ_E value as found by the T/D ratio between liquid and gas at test 12 (11:00 A.M. on April 12). The mean value over all the cells except for cell 8 was $\approx(300/150) = 2$.

From the data shown so far, it is possible to evaluate the ratio between the nuclear products found, i.e., tritium and neutrons. The experimental knowledge of the d-d reaction in vacuum is limited to a minimum energy of ~10 keV, and the ratio of the two channels [Eqs. (8) and (9)] is practically unity.

In our case, the ratio of tritium atoms to neutrons is given by the following equation by taking into account that the main count rate changes occurring in a time interval starting from time τ and lasting ~8 h:

$$T/n = k\left(\sum_i T_i\right)\Big/C \ , \qquad (11)$$

where

T = tritium atoms in excess of the electrolytic enrichment

n = number of neutrons

$\sum T_i$ = summation of the tritium excess (decay/min·ml) in all the cells where the excess was found

C = change of the neutron count in the considered time interval Δt

k = constant, the value of which is 1.42×10^4 decay/min·ml, given by the relation

$$k = \mathcal{N} f V_0 / c_1 c_2 \mathfrak{A} m_T \ , \qquad (12)$$

where

$\mathcal{N}$ = Avogadro's number

f = efficiency of the neutron counter = 5×10^{-5} count/neutron

c_1 = constant for the conversion from decays per minute to decays per second = 60

c_2 = constant for the conversion from curies to decays per second = 3.7×10^{10}

$\mathfrak{A}$ = tritium specific activity = 9.8×10^3 Ci/g

m_T = tritium atomic weight = 3.014.

Figure 9a shows the count rate and the integral count recorded in the period between 10:45:58 on May 15 and 20:02:10 on May 18 in which both tests 21 and 22 were done. As already discussed, because of the nature of the signals generated in that period, the integral count was different according to the working frequency of the counter utilized. We found the values 150, 350, and 667, respectively, at 500 Hz, 400 kHz, and 125 MHz as changes in the neutron counts in Δt (see Fig. 9b). The $\sum T_i$ can assume two values, 1067 and $\approx$6000, respectively, if the experimental or calculated value at time τ [Eq. (10)] is considered.

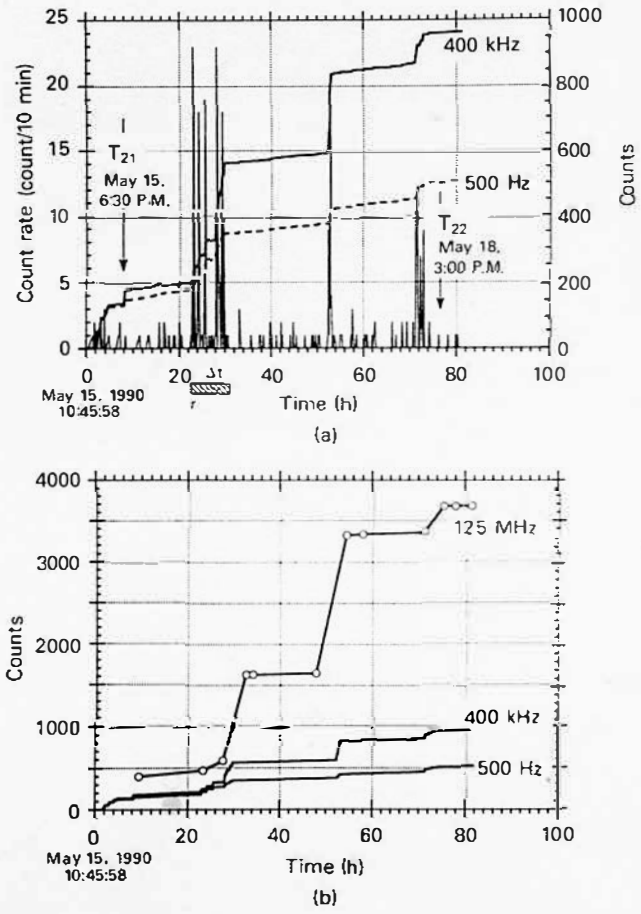

Fig. 9. Acquisition of the neutron emission in the time interval within tritium tests 21 and 22: (a) count rate and count and (b) comparison of the counts obtained by the three counters.

Therefore, the T/n ratio can be considered within the values

$$k\left(\sum_i T_i\right)_{min}\Big/C_{125\ MHz} < (T/n) < k\left(\sum_i T_i\right)_{max}\Big/C_{500\ Hz}$$

or

$$(2.27 \pm 0.03) \times 10^4 < (T/n) < (5.7 \pm 0.3) \times 10^5 \ , \qquad (13)$$

in which the most conservative value is

$$k\left(\sum_i T_i\right)_{min}\Big/C_{500\ Hz} = (1.0 \pm 0.1) \times 10^5 \ .$$

The error on the T/n ratio is given by

$$\Delta(T/n) = \left|(k/C)\left(\sum_i \Delta T_i - \sum_i T_i\sqrt{C}/C\right)\right| \ ,$$

where ΔT_i is the absolute error on the tritium measurement given automatically by the instrument as 2σ%, and the Poisson's distribution for the neutron count was taken into account. Throughout the experiment, this value was practically constant at around ±20 decay/min·ml.

In an experiment carried out in April 1989 (Ref. 5), we found an excess of tritium atoms equal to $(2.14 \pm 0.04) \times 10^{11}$ and a neutron emission of 7.2×10^5 in 240 s. These data can

be now compared with those reported in this technical note. The earlier T/n ratio was $(2.97 \pm 0.06) \times 10^5$ which does not differ appreciably from the value calculated with Eq. (13), which is between the most conservative and the maximum value. The mean number of tritium atoms produced in each of the three cells in the current experiment was $(1.01 \pm 0.06) \times 10^{11}$ if we refer to the experimental value, whereas it becomes 5.7×10^{11} if we refer to the calculated value [Eq. (10) and Fig. 8]. The count rate observed earlier was 0.15 count/s, which is comparable with the values here reported.

Thermal Effects

Concerning thermal effects, it is necessary to point out that our system did not allow measurement of excess heat. Work is in progress to overcome this problem. In this technical note, we describe some experimental evidence that would require further investigation by calorimetry.

Unlike the Fleischmann-Pons experiment in which the temperature was measured in the electrolytic solution, we measured the temperature of the cathode itself. In this way, we avoided the problems related to the thermal gradients in the solution, which were a source of criticism against the Fleischmann-Pons work[1] and efforts to defend those data.[17] Furthermore, direct measurement of the electrode temperature allows instantaneous detection, with better sensitivity, of thermal effects associated with processes occurring both in the bulk and on the surface. On the other hand, the interpretation of the temperature data is more complex. In fact, unlike the Fleischmann-Pons calorimeter, in which the temperature of the solution is proportional to the difference between the input power and the output power, in our case the temperature of the electrode also depends on the joule power produced across the electrode. An effect equal to I^2R is generated by the current I crossing the cathode of resistance R. An increase of R during an experiment at I = constant immediately produces an increase of the electrode temperature T_i and then an increase of temperature of the solution. A sudden increase of R, and consequently of T_i, can result from morphological modifications of the electrode (dislocations, fractures, nucleation of new phases, etc.) due to the absorption of deuterium. If this is observed to be correlated to other independent experimental variables, such as neutron emission or tritium production, the measured thermal effect supports the detection of nuclear particles, but if they are absent, the thermal effect is not proof of nuclear processes in the bulk or on the surface.

The temperature of the cathode at a given current I is the result of other contributions, in addition to the one already discussed, due to both the overall cathodic process

$$D_2O + e(Pd) = D_{ads} + OD^- \quad (14a)$$

$$D_{ads} + D_{ads} = D_2(g) \quad (14b)$$

$$D_2O + D_{ads} + e(Pd) = D_2(g) + OD^- \quad (14c)$$

and

$$D_{ads} = D(Pd) \quad (14d)$$

localized on the surface and the thermal exchanges with the electrolyte and current lead (thermocouple shield in the present case).

If the cathode were partially dipped into the solution, two effects, completely different by nature but both exothermal, would occur: (a) increase of the cathodic overvoltage η_c due to the increase of the current density following the reduced area of the cathode/electrolyte interface and (b) catalytic recombination of deuterium (palladium) with O_2.

Consider now the following reasoning based on the comparison of the energy balance in the i'th cell and cell 8 in H_2O. For the i'th cell in D_2O, the energy balance is

$$I|\Delta V_i| + P_i = IE_D + \mathfrak{D}_i \ , \quad (15)$$

and the energy balance in H_2O becomes

$$I|\Delta V_H| = IE_H + \mathfrak{K} \ , \quad (16)$$

where

P_i = excess of energy

E_D, E_H = voltage corresponding to thermoneutrality for D_2O and H_2O decomposition, respectively, which is given by $\Delta_f H^0/2$ F

$\Delta_f H^0$ = corresponding formation standard enthalpy.

The terms $\mathfrak{D}_i$ and $\mathfrak{K}$ are defined by

$$\mathfrak{D}_i = \left(\sum_j w_j\right)_{D_2O}$$

and

$$\mathfrak{K} = \left(\sum_j w_j\right)_{H_2O} \ , \quad (17)$$

and they represent all the possible heat exchange terms (cell and thermostated bath, electrolyte and gas, electrodes and their leads), which are the output power from the cell.

The difference between Eqs. (15) and (16) is

$$P_i = I(\Delta E - |\Delta V_i| + |\Delta V_H|) + (\mathfrak{D}_i - \mathfrak{K}) \geq 0 \ , \quad (18)$$

where

$$\Delta E = E_D - E_H = 1.527 - 1.481 = 0.046 \ V \quad \text{at } 298 \text{ K} \ .$$

In our case, the difference $(\mathfrak{D}_i - \mathfrak{K})$ is unknown. A qualitative evaluation can be done by assuming this term to be either a constant or a function of the input power. If we write Eq. (18) in the form

$$[\Delta E + (|\Delta V_H| - |\Delta V_i|)] \geq (\mathfrak{K} - \mathfrak{D}_i)/I \ , \quad (19)$$

this allows us to represent the left term, which is completely experimental, as a function of current I.

Some comments should be made regarding this approach:

1. The cells in D_2O and the one in H_2O are equal in the volume and nature of the materials contained.

2. Because all the cells are connected in series, by Faraday's law, this implies that the gas flow rate outcoming from each cell must be the same. The heat carried by this gaseous flux is not the same. In fact, the specific heat of D_2 is 1.3% greater than that of H_2. Furthermore, this flux has to be saturated by water at the temperature of the electrolyte solution removing a heat quantity on time given by

$$I(\lambda + C_p\Delta T)/2 \text{ F} \ ,$$

where

λ = latent heat of evaporation of D_2O or H_2O

C_p = specific heat

ΔT = temperature difference between the gas flux and the electrolyte solution.

The difference between the two terms produces the quantity

$$[(\lambda_H - \lambda_D) + (C_{p,H} - C_{p,D})\Delta T]I/2\,F \ .$$

Since the differences in the parentheses are both negative, the sign of the term that contributes to the difference $(\mathfrak{IC} - \mathfrak{D}_i)$ depends on ΔT, and it is proportional to the applied current.

3. The geometric arrangement of the cells (see Fig. 1) is such as that the heat exchanged with the thermostatic bath is equal for all the cells if the temperature difference between each cell and bath, at temperature T_b, is the same. By considering that the cell holder, made of Pyrex, has a surface area of 77 cm^2, a thickness of 0.2 cm, and thermal conductivity at 273 K of 1.1×10^{-2} $J(cm \cdot s \cdot K)^{-1}$, for $\Delta T = 1$ K, the power exchanged is ≈4 W. Therefore, the contribution to the difference $(\mathfrak{IC} - \mathfrak{D}_i)$ is null if the comparison with the cell in H_2O is done with the cells at the same temperature.

4. The physical and geometrical characteristics of the electrode/lead junctions are practically the same in the limits of a handwork done with great accuracy. Therefore, the heat exchanged by the electrodes does not contribute to the difference $(\mathfrak{IC} - \mathfrak{D}_i)$ if the electrodes of the cells compared are maintained at the same temperature.

Figure 10 shows the application of Eq. (19) to some cells. The quantity $[\Delta E + (|\Delta V_H| - |\Delta V_i|)]$ is represented by the term $K - \Delta V_i$. At high currents, the term $(\mathfrak{IC} - \mathfrak{D}_i)$ is no longer constant as it is at lower currents, where its value is practically zero. This behavior displays a predominant role of the terms depending on I or I^2 on the difference $(\mathfrak{IC} - \mathfrak{D}_i)$.

Figure 11a shows the trend of the cathode temperature of the cells 1, 2, and 3 in the period during which the neutron count rate markedly increased and a tritium excess was measured. The data acquisition shows that there was a certain degree of correlation with the neutron emission.

Figure 11b shows the same type of plot, but in this case, the thermal behavior is referred to the cathode of cell 6. The temperature started to increase while the neutron emission was occurring, reaching 80°C. It was necessary to manually add heavy water to compensate for the loss by evaporation. Since we did not find a tritium excess in that cell and we were not able to localize the direction of the neutron emission, we cannot give any experimental explanation for the phenomenon. We may suppose that an event occurred that changed the resistance of the cathode in ~6 h, increasing the I^2R effect and, consequently, its temperature. The fracture propagation and/or substantial D_2 desorption localized in the close porosity of the cathode are events that could justify an increase in R. According to some authors, cold fusion events could be originated just by those phenomena.

For the same period, Fig. 12 shows the recording of the temperature of the cathode of cell 6 compared with the input power $I|\Delta V_6|$, where a strict correlation clearly appears. To obtain a comparative view, the curves of the temperature of cell 8 in H_2O and thermostat T_b, were reported. The manual addition of D_2O in cell 6 produced only a momentary decrease of the temperature of the electrolytic solution and, consequently, a decrease of the quantity I^2R. As shown in Fig. 12, T_b was constant, and nothing to be compared occurred in cell 8 or in the other cells (note that the current was equal for all the cells so that the comparison of the input power has to be done by the term $|\Delta V_i|$).

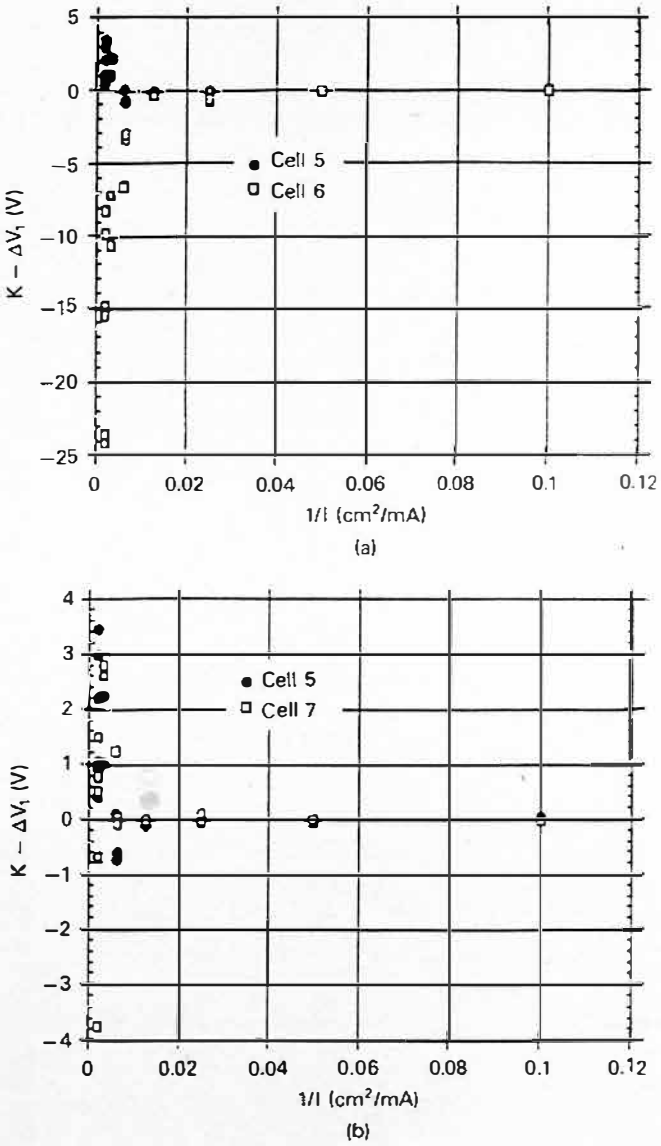

Fig. 10. Use of Eq. (21): (a) comparison of cells 5 and 6 and (b) comparison of cells 5 and 7. The quantity $\Delta E + (|\Delta V_H| - |\Delta V_i|)$ in Eq. (19) is represented by the term $K - \Delta V_i$.

Gamma Radiation Measurements

The gamma radiation measurements recorded by the two detectors during the period when the neutron count rate increased and tritium excess was found did not show any significant change with respect to the natural background.

What is expected to be found as a consequence of the neutron emission in a medium containing a high concentration of protons (light water in the thermostat) is the emission of 2.225-MeV gamma photons caused by the reaction $n + p = d + \gamma$.

Through measurements performed to calibrate the apparatuses by using Am-Be neutron sources of different activities positioned in place of the cells, we could calculate that

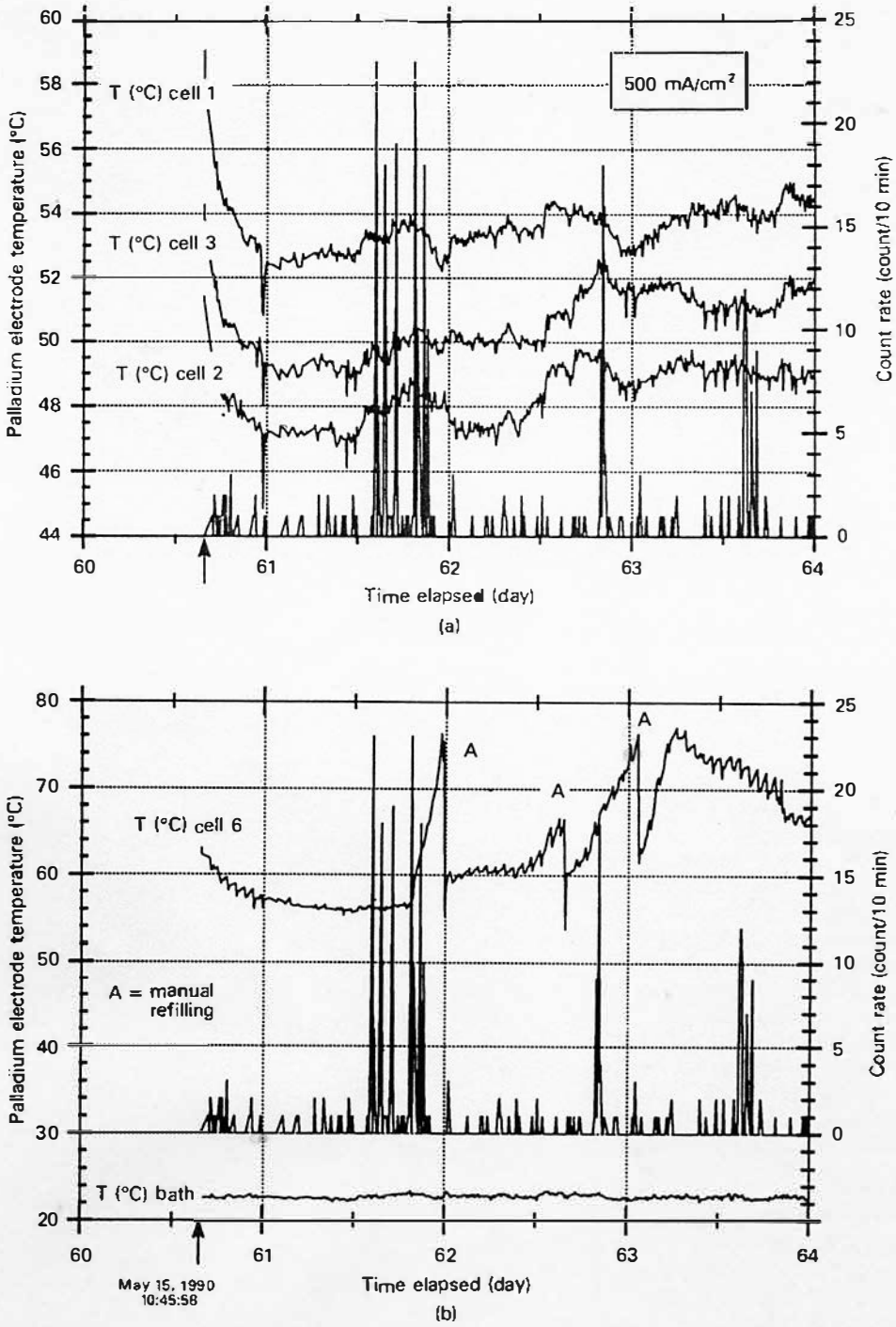

Fig. 11. Electrode temperatures for some cells in the period when the tritium excess and neutron emission was detected: (a) cathode temperatures and neutron count rates of cells 1, 2, and 3, which gave tritium excess, and (b) cathode temperature and neutron count rate of cell 6 compared with the temperature of the thermostated bath water (points labeled A show the manual addition of D_2O to replenish the electrolytic solution).

the neutron emission observed, even if concentrated in only one gamma acquisition period lasting 24 min, would have not been suitable to produce sufficient gamma radiation to be detected also by the detector closest to the cell source of neutrons. Therefore, we are led to conclude that the measurement of the gamma spectrum at the present level of sensitivity is not inconsistent with the estimated neutron emission.

CONCLUSIONS

The results given in this technical note show three significant experimental results, two of which are of nuclear origin. They are as follows:

1. A substantial increase in the neutron count rate was observed after ~60 days of continuous experimentation. The

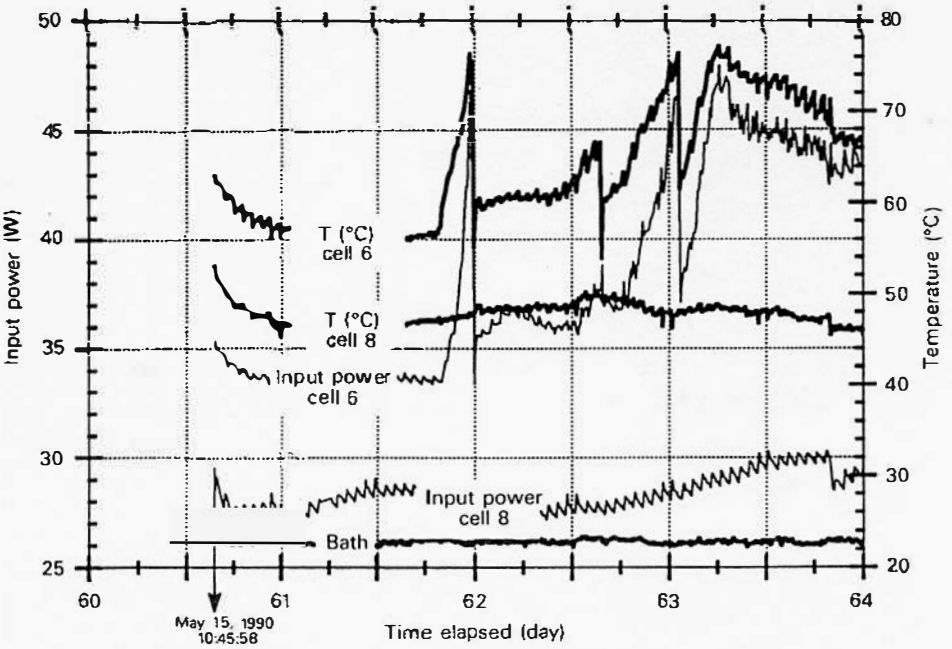

Fig. 12. Temperature and input power compared for cells 6 and 8 (H_2O).

phenomenon showed a discontinuous trend with a burst structure that lasted for ~10 days, and it seemed to be correlated with the value of the electrolysis current density applied to the ten cells connected in series. There are some indications in our experimental conditions that a threshold does exist at ~320 mA/cm^2. The pulse-shape discrimination of the signals coming from the neutron detector did not allow us to obtain the dating and shape of all the signals counted. Therefore, we cannot claim that the observed phenomenon was exclusively nuclear by nature. Our presence in the laboratory during that period allowed direct observation of the behavior of the emission events. The characteristic time sequence and the number of counts per burst were very typical and not comparable with simulated electromagnetic noise randomly induced on the neutron counter, which was not previously observed in ~1 yr of background recording.

2. Tritium excess in three cells out of nine (one cell out of ten worked in light water) was found to be equal to about twice the maximum value expected by the electrolytic enrichment and about four times the initial value of the tritium activity. This result was found in the period during which the increase of the neutron count rate was observed, when the current density applied was at its highest value. If we assume that the tritium production occurred in a very short time with respect to the interval between one tritium test and the next one, the calculated value of the tritium activity, on the basis of the tritium mass balance equation, at the time corresponding to the increase of the neutron emission, was more than five times greater than the expected value. We are confident about these results because we systematically performed >350 tritium analyses that were always in agreement, within the experimental error, with the calculated values, and, as other sources of error can be excluded, we believe that a nuclear process was really occurring in those cells.

3. The palladium cathodes that gave tritium production were prepared in a different way from the other cathodes. We cannot say if what we did is really correlated with our findings because a series of investigations is still in progress and further experimentation has to be done. However, the X-ray diffraction patterns of the electrodes show characteristic and well-defined modifications that are correlated to the preparation procedure.[18] Even if they belonged to two different groups, we suppose them to be highly dislocated.

Finally, there seems to exist a good internal consistency in our results concerning the tritium production, the tritium/neutron ratio, and the neutron count rate.

Although some anomalous thermal effects were observed, we cannot compare them to previous results or correlate them with the energy excess because the experimental system did not allow a calorimetric measurement.

From the experimental and scientific point of view, we are at a point where a quality improvement of the experimentation is required in order to contribute effectively to the scientific development of this matter. It is no longer sufficient merely to observe events of a phenomenon for which we do not know the cause or time of occurrence. We believe it is necessary to apply the experimental strategies of nuclear and calorimetric detection as well as to determine other physicochemical variables that may drive the reaction. We believe that our efforts now have to be concentrated on two aspects: (a) improvement, mainly qualitative, of the neutron detection and (b) *design* of the cathode based on the fundamentals of material science.

Some researchers claim that neutron detection is reliable if more detectors are present in the laboratory. In principle, this is certainly true, but we believe that pulse-shape analysis has to be mandatory when proportional counters are used. It needs to date, discriminate, and store all the pulse shapes of the signals that are counted. We are moving to do this through a recently ordered neutron counter that will be produced by JOMAR to host our ten-cell system. It is an up-to-date counter equipped with 60 ^{3}He tubes and a shift register.

Signal shape information will be stored. We hope it will be possible to complete it with a fast data acquisition and pulse-shape discrimination system to perform the measurements accordingly.

In terms of cathode design, we mean the ideation of one or more treatments capable of giving to the material particular structural, physicochemical, and mechanical properties. This has to be seen in terms of producing a material that behaves according to our working hypothesis as recently reported in the literature.[19]

In concluding this technical note, we believe that the time is ripe for research on the nuclear process in condensed matter to be considered in the same fashion as other research that does not yet have well-consolidated theories behind it, that does not yield routinely reproducible results, that does not yet have complete acceptance by the scientific community, that will not produce useful energy at least in the near future, and so on, but are financed and studied with the aim to understand.

ACKNOWLEDGMENTS

The authors are very grateful to both E. Cardarelli for lithium measurements by induction-coupled plasma atomic absorption spectroscopy and P. Porta for high-resolution X-ray diffraction measurements on palladium electrodes.

This work was partially supported by the Fusion Programme of the European Community through contract 387/89-7/FUA I. The National Research Council contributed financially to the realization of a dedicated laboratory, and the Physics Laboratory of the Istituto Superiore di Sanità as well as the National Institute of Nuclear Physics, Sezione Sanità, and Università "La Sapienza" gave their support both financial and in terms of nuclear instrumentation, staff, and space in the Department of Chemistry where the experimental activity was carried out.

REFERENCES

1. M. FLEISCHMANN and S. PONS, "Electrochemically Induced Nuclear Fusion of Deuterium," *J. Electroanal. Chem.*, **261**, 301 (1989); see also Errata, *J. Electroanal. Chem.*, **263**, 187 (1989).

2. S. E. JONES et al., "Observation of Cold Nuclear Fusion in Condensed Matter," *Nature*, **338**, 737 (1989).

3. S. FRULLANI and D. GOZZI, seminars presented at INFN-ENEA, Frascati, Italy, May 4, 1989, and Dipartimento di Chimica, Università "La Sapienza," Rome, Italy, May 16, 1989.

4. D. GOZZI et al., "Nuclear and Thermal Effects During Electrolytic Reduction of Deuterium at Palladium Cathode," *J. Fusion Energy*, **9**, 241 (1990).

5. D. GOZZI et al., *Nuovo Cimento*, **103A**, 143 (1990).

6. D. GOZZI et al., "Fusione Nucleare Fredda a Confinamento Chimico: Quali Certezze?," presented at Milan, Italy, July 11, 1989.

7. S. FRULLANI et al., "Understanding of Cold Fusion Phenomena," *Proc. Workshop Understanding of Cold Fusion Phenomena*, Varenna, Italy, September 15-16, 1989.

8. D. GOZZI et al., presented at LXXV Congress SIF, Cagliari, Italy, September 28-October 3, 1989.

9. G. H. LIN, R. C. KAINTHLA, N. J. C. PACKHAM, O. VELEV and J. O'M. BOCKRIS, *Int. J. Hydrogen Energy*, **15**, 537 (1990); N. J. C. PACKHAM, K. L. WOLF, J. C. WASS, R. C. KAINTHLA, and J. O'M. BOCKRIS, "Production of Tritium from D_2O Electrolysis at a Palladium Cathode," *J. Electroanal. Chem.*, **270**, 451 (1989).

10. F. J. MAYER, J. S. KING, and J. R. REITZ, "Fusion in from the Cold?," *J. Fusion Energy*, 9, 241 (1990); see also H. O. MENLOVE et al., "Measurement of Neutron Emission from Ti and Pd in Pressurized D_2 Gas and D_2O Electrolysis Cells," *J. Fusion Energy*, 9, 495 (1990); P. K. IYENGAR and M. SRINIVASAN, "Overview of BARC Studies in Cold Fusion," *Proc. 1st Annual Conf. Cold Fusion*, Salt Lake City, Utah, March 28-31, 1990, p. 62; F. SCARAMUZZI et al., "Search for Nuclear Phenomena by the Interaction Between Titanium and Deuterium," *Proc. 1st Annual Conf. Cold Fusion*, Salt Lake City, Utah, March 28-31, 1990, p. 17; S. E. JONES, "Anomalous Neutron Emission in Metal-Deuterium Systems," *Proc. Conf. Muon-Catalyzed and Cold Fusion*, Riken, Japan, November 1989.

11. G. H. LIN, R. C. KAINTHLA, N. J. C. PACKHAM, and J. O'M. BOCKRIS, "Electrochemical Fusion: A Mechanism Speculation," *J. Electroanal. Chem.*, **280**, 207 (1990).

12. S. K. MALHOTRA, M. S. KRISHNAN, and H. K. SADHUKHAN, "Material Balance of Tritium in Electrolysis of Heavy Water," in "BARC Studies in Cold Fusion," P. K. IYENGAR and M. SRINIVASAN, Eds., BARC-1500, Bhabha Atomic Research Centre (1989).

13. G. TAUBES, "Cold Fusion Conundrum at Texas A&M," *Science*, **348**, 1299 (1990).

14. T. N. CLAYTOR et al., "Tritium and Neutron Measurements of a Solid State Cell," preprint LAUR-89-39-46, Los Alamos National Laboratory; P. G. SONA et al., "Preliminary Tests on Tritium and Neutrons in Cold Nuclear Fusion Within Palladium Cathodes," *Fusion Technol.*, **17**, 713 (1990); C. D. SCOTT et al., "A Preliminary Investigation of Cold Fusion by Electrolysis of Heavy Water," ORNL/TM-11322, Oak Ridge National Laboratory (Nov. 1989); R. R. ADZIC et al., "Tritium Measurements and Deuterium Loading in D_2O Electrolysis with a Palladium Cathode," *Proc. 1st Annual Conf. Cold Fusion*, Salt Lake City, Utah, March 28-31, 1990, p. 261; J. CHÉNE and A. M. BRASS, "Tritium Production During the Cathodic Discharge of Deuterium on Palladium," *J. Electroanal. Chem.*, **280**, 199 (1990).

15. E. STORMS and C. TALCOTT, "Electrolytic Tritium Production," *Fusion Technol.*, **17**, 680 (1990).

16. J. O'M. BOCKRIS, G. H. LIN, R. C. KAINTHLA, N. J. C. PACKHAM, and O. VELEV, "Does Tritium Form at Electrodes by Nuclear Reactions?," *Proc. 1st Annual Conf. Cold Fusion*, Salt Lake City, Utah, March 28-31, 1990, p. 137.

17. S. PONS and M. FLEISCHMANN, "Calorimetry of the Palladium-Deuterium System," *Proc. 1st Annual Conf. Cold Fusion*, Salt Lake City, Utah, March 28-31, 1990, p. 1; see also *Fusion Technol.*, **17**, 669 (1990).

18. D. GOZZI et al., Unpublished.

19. M. TOMELLINI and D. GOZZI, "On the Possibility for Local Oversaturation of Deuterium in Palladium," *J. Mat. Sci. Lett.*, **9**, 836 (1990).